Thick and anisotropic D” layer beneath Antarctic Ocean

Yusuke Usui, Yoshihiro Hiramatsu and Muneyoshi Furumoto

Graduate School of Natural Science and Technology, Kanazawa University

Kakuma, Kanazawa, 920-1192, Japan

Masaki Kanao

Natural Institute of Polar Research

1-9-10 Kaga, Itabashi-ku, Tokyo, 173-8515, Japan

Abstract. Waveform modeling and travel times analyses of S, ScS and SKS phases recorded at the broad-band permanent station SYO in the Antarctic are used to determine the shear wave velocity structure and transverse isotropy in the D” layer beneath the Antarctic Ocean. The SH wave structure has a discontinuity with the velocity increase of 2.0% at 2550 km. The SV structure is similar to PREM model. The magnitude of the anisotropy is highest at the top of D” layer and lowest at the core-mantle boundary. The D” layer beneath the Antarctic Ocean is significantly thicker than those beneath Alaska and the Caribbean Sea. We attribute this anisotropic D” layer to paleo-slab materials. The subduction in and around the Antarctic Ocean has started ~180Ma and is the one of the oldest in the world. It has provided a large amount of the slab materials in the lowermost mantle.

Introduction

A bottom layer with a thickness of several hundred kilometers in the mantle has been recognized to be anomalous in comparison with the overlying mantle since the classification of the D” region by Bullen [1949]. Recently, seismological analyses of a huge amount of data have revealed various properties of the D” layer. The shear wave velocity increases 2-3 % at the top of the D” layer and has a negative velocity gradient in the D” layer beneath some regions, Alaska [Young and Lay, 1990], the Caribbean Sea [Lay and Helmberger, 1983], and India [Young and Lay, 1987], where global tomographic models show high velocity anomalies in the lowermost mantle. On the other hand, a low velocity anomaly region beneath the Central Pacific has no discontinuity but strong negative velocity gradient in the D” layer [Ritsema and Garnero, 1997]. Furthermore, ultra-low velocity zones with 5-10% decrease of P wave velocity exist in some parts above the CMB [Garnero and Helmberger, 1998].

Anisotropy of the shear wave velocity is another characteristics of the D” layer. The D” layer beneath Alaska and the Caribbean Sea regions show shear wave anisotropy [Kendall and Silver, 1996; Garnero and Lay, 1997]. S waves passing through the D” layer beneath these regions show arrivals of longitudinal (SV) components several seconds later than those of the transverse (SH) components, indicating that there is a 2-3% velocity difference between SV and SH waves. The anisotropy of the shear wave velocity is the transverse isotropy with vertical axis of the symmetry [Kendall and

Silver, 1996; Matzel et al., 1996; Kendall, 2000]. The transverse isotropy may be generated by the strain field of horizontal mantle flow at the base of the mantle.

The global mapping of both the heterogeneity and the anisotropy of the shear wave velocity in the lowermost mantle helps us to understand the dynamics of the whole mantle (i.e., mantle convection). However, because data from many seismic stations were used in previous work, the analyses of the velocity structure in the D” layer were performed mainly on the northern hemisphere. To circumvent such a spatial limitation, we apply a single station analysis using sources as a signal source array. Recent high quality broad-band waveform data at a single station enable us to construct the shear wave velocity model in the D” layer on the southern hemisphere that has seldom been reported before. We have investigated the anisotropy of the shear wave velocity in the D” layer beneath the Antarctic Ocean, off the south coast of Australia, using the records at the Syowa station in Antarctica and discuss what determines the thickness of the D” layer.

Data

We examine seismograms recorded by STS-1 broad-band seismographs at the Syowa station in Antarctica from 1990 to 2001. We select events whose source depths are from 113 to 623 km to reduce the effects of source-side heterogeneity and anisotropy. We use large events whose magnitudes are between 5.7 and 7.6 to obtain high quality signals. The required source-receiver distance ranges 85°-95° and the slowness ranges 8.7s/deg - 9.6s/deg. Figure 1 shows the locations of used 13 deep earthquakes in the south Pacific subduction zones.

We apply two corrections to the observed waveforms before the analysis of S, ScS and SKS waves, removing the effects of the upper mantle anisotropy beneath the station [Kubo and Hiramatsu, 1998] and the heterogeneity of the shear wave velocity in the upper- and mid-mantle. For the first correction, we estimate SKS splitting parameters, the direction of the fast-polarized wave and the delay time between the fast and slow polarized waves [Silver and Chan, 1991]. The estimated SKS splitting parameters are consistent with those reported by Kubo and Hiramatsu [1998] and independent of source locations, indicating little effect of the upper mantle anisotropy of source-side in the following analysis. The corrected travel times are about one second for each event. Then we correct the waveform using the obtained parameters. As the second correction, we correct the travel time anomalies due to the shear wave velocity heterogeneity in the upper- and mid-mantle along ray paths using the 3-D velocity model (Model S16U6L8) by Liu & Dziewonski [1998]. These corrections amount to -0.6s for SKS waves, -0.9s for ScS waves and -3.5s for S waves.

We transform the waveforms recoded by the two horizontal components into SH and SV components of the shear wave signals. The time delay between SV and SH arrivals on the separated components is measured by picking the onsets of the signals.

The measurement picking error is ±0.2s.

Construction of shear wave velocity structure

Differential travel times of the split S waves are up to 4s, and show that SH energy arrives earlier than SV energy (Figure 2). The absence of significant splitting of S waves with turning points shallower than 450 km above the CMB and the increase in differential travel times with the decrease of slowness confirm that anisotropy is localized in the lowermost mantle. We calculate synthetic waveforms using the Direct Solution Method [DSM: Cummins et al., 1994; Takeuchi et al., 1996], the P-SV systems is decoupled from the SH systems in DSM, and we construct the velocity structure in the D” layer which explains the observed waveforms and SKS-S and ScS-S differential travel times. We assume that the velocity structure is identical to PREM [Dziewonski and Anderson, 1981] from the structure down to 2000 km and deviates from PREM up to ±0.5% from the depth of 2000 km to the top of the D” layer. In the D” layer, we assume that the SV structure is PREM-like while the SH has a velocity discontinuity at the top of the D” layer because the observed waveforms show double arrival (Figure 3) due to D” discontinuity as some other regions [Lay and Helmberger, 1983; Young and Lay, 1987, 1990].

We focus on velocity discontinuity at the top of D” layer for SH in the searching best-fit model. Modifying the depth of the discontinuity in a range 2500km ~

2700km with an interval of 50 km, the velocity jump 1.0% ~ 3.0% with an interval of 0.5% and the velocity at CMB -0.5% ~ +0.5% with an interval of 0.25% around PREM, we search an optimum SH velocity structure under the given set of conditions. Figure 3 displays examples of three different velocity discontinuity models. Synthetic waveforms show that the shallower discontinuity with small velocity jump and the deeper discontinuity with large velocity jump are not able to explain both the S arrival time and the pulse shape of the secondary phase. On the other hand, the model of the discontinuity at 2550km with 2% velocity jump reproduces those well. This is also supported by the fact that the discontinuity at 2550km with 2% velocity jump shows the minimum root mean square (RMS) of SKS-S differential travel time residuals in the searching range.

Finally we construct the optimum transverse isotropic model (hereafter referred as SYYM model, Figure 3) which explain well the observed differential travel times and waveforms (Figure 2 and 3). SYYM-SH model contains a 2.0% velocity discontinuity at a depth of 2550 km and a negative velocity gradient in the D" layer. SYYM-SV model has the same structure as PREM down to a depth of 2741 km and a positive velocity gradient in a depth range of 2741 km to the CMB. The velocities of SH and SV waves are 0.25% faster than those expected from PREM at the CMB (Figure 3).

We also try to construct no discontinuity models for SH (i.e. steep velocity gradient models). However, the differential travel times and the pulse shape of S waves of the no discontinuity models are inferior to those of the discontinuity models. We, therefore, consider that the optimum model is the discontinuity model as shown in Figure 3 although a lateral variation of shear wave velocity structure in the D” layer may cause some trade-off between the sharpness and the depth of the discontinuity.

Discussion

SYYM model shows a 2.0% velocity discontinuity of SH at the depth of 2550km and both SV and SH waves have velocities higher than those of PREM at the lowermost mantle. SYYM model is consistent with the high velocity anomaly in the region at the lowermost mantle reported by global tomographic studies [Kuo et al., 2000; Masters et al., 2000; Liu and Dziewonski, 1998] and a radial anisotropic model obtained by a global waveform tomography [Panning and Romanowicz, 2004]. The seismic features are the same as those reported for the D” layers beneath Alaska [Garnero and Lay, 1997; Matzel et al., 1996] and the Caribbean Sea [Kendall and Silver, 1996] where the velocity structure of shear wave in the D” layer is well resolved.

The transverse isotropy D” layer with high velocity anomaly is possibly caused by the lattice preferred orientation in the slab material descending into the lower mantle [Kendall and Silver, 1996; Garnero and Lay, 1997]. In the Antarctic Ocean region, Richards and Engebretson [1992] propose that the subduction has started ~180Ma, indicating the anisotropy of shear wave velocity can be attributed to the paleo-slab material in the D” layer beneath the Antarctic Ocean.

The D” layer beneath the Antarctic Ocean is by much thicker than those beneath the other regions. The thickness of the D” discontinuity beneath Alaska and the Caribbean Sea are about 250 km (SYLO and SLHE models in Figure 3), which is nearly 100 km thinner than the D” layer beneath the Antarctic Ocean. The cause for the difference in the thickness of the D” layer may be the difference in the subduction history. The oldest and the most persistent subduction exists in and around the Antarctic Ocean region (180 Ma to the present), while Alaska and the Caribbean Sea regions have younger subductions which started the 90~120 Ma [Richards and Engebretson, 1992]. Thus, accumulation of the paleo-slab material beneath the Antarctic Ocean is more than those beneath Alaska and the Caribbean Sea. The variation in the thickness of the D” layer for regions with $V_{SH} > V_{SV}$ is controlled by the amount of deposited paleo-slab materials. Recently Tsuchiya et al. [2004a] reported a phase transition in $MgSiO_3$-perovskite at the lowermost mantle pressure-temperature condition and Post-perovskite $MgSiO_3$ was anisotropic, producing maximum 10 % transverse isotropy [Tsuchiya et al., 2004b]. The oldest subduction may decrease the temperature in the lowermost mantle beneath the Antarctic Ocean. A positive Clapeyron slope of the phase transition in $MgSiO_3$ perovskite [Tsuchiya et al., 2004a] is a possible cause to control the difference in the thickness of D” the layer.

Conclusions

S waveform data recorded at the Syowa station in Antarctica are used to investigate the fine structures of D” anisotropy in the lowermost mantle beneath the Antarctic Ocean. We construct a new transversely isotropic shear wave velocity model (SYYM) for the D” layer in the region. SYYM-SH velocity structure contains a 2.0% increase in the velocity at the top of D" layer, about 350km above the CMB. SYYM-SV structure is similar to PREM model. The anisotropic D” layer of this region is thicker than those beneath Alaska and the Caribbean Sea regions. Combination of the thickness of anisotropic D” layer and the subduction histories suggests that the variation of D" thickness is related to the amount of paleo-slab material deposited on the CMB.

Acknowledgements

We are grateful to Nozomu Takeuchi for providing us the source code of DSM. We also thank Satoru Tanaka for providing us the code to calculate travel time anomaly. The comments of two anonymous reviewers are useful in improving our manuscript.

References

Bullen, K. E. (1949), Compressibility-pressure hypothesis and the Earth’s interior, *Mon. Not. R. astr. Soc, 5*, 355-368.

Cummins, P. R., R. J. Geller, T. Hatori, and N. Takeuchi (1994), DSM complete synthetic seismograms: SH, spherically symmetric case, *Geophys. Res. Lett.*, *21*, 533-536.

Dziewonski, A. M., and D. L. Anderson (1981), Preliminary reference earth model, *Phys. Earth. Planet. Inter, 25,*297-356.

Garnero, E. J., and D. V. Helmberger (1998), Further structural constrains and uncertainties of a thin laterally varying ultralow-velocity layer at the base of mantle, *J. Geophys. Res*., *103*, 12495-12509.

Garnero, E. J. and T. Lay (1997), Lateral variations in lowermost mantle shear wave anisotropy beneath the north Pacific and Alaska, *J. Geophys. Res*., *102*, 8121-8135.

Kendall, J. M. and P. G. Silver (1996), Constrains from seismic anisotropy on the nature of the lowermost mantle, *Nature*, *381*, 409-412.

Kendall, J. M. (2000), Seismic anisotropy in the boundary layers of the mantle, *earth's deep interior, AGU Geophys. monograph*, S. Karato (ed.), *117*, 133-155.

Kubo, A. and Y. Hiramatsu (1998), On presence of seismic anisotropy in the Asthenosphere beneath continents and its dependence on plate velocity: Significance of reference frame selection, *Pure appl. geophys*., *151*, 281-303.

Kuo, B.Y., E.J. Garnero, and T. Lay (2000), Tomographic Inversion of S-SKS times for shear wave velocity heterogeneity in D'': Degree 12 and hybrid models, *J.*

Geophys Res., *105*, 28139-28157.

Lay, T., and D. V. Helmberger (1983), A lower mantle S-wave triplication and the shear velocity structure of D”, *Geophys. J. R. astr. Soc, 75*, 799-837.

Liu, X. -F. and A. M. Dziewonski (1998), Global analysis of shear wave velocity anomalies in the lower-most mantle, in *The Core-Mantle Boundary Region*, M. Gurnis, M. E. Wysession, E. Knittle, B. A. Buffet, Eds. (American Geophysical Union, Washington, DC), pp. 21-36.

Masters, G., Laske, G., Bolton, H., and Dziewonski, A. M. (2000), The relative behavior of shear velocity, bulk sound speed and compressional velocity in the mantle: Implications for chemical and thermal structure, *earth's deep interior, AGU Geophys. monograph,* S. Karato (ed.), *117,* 133-155.

Matzel, E., M. K. Sen and S. P. Grand (1996), Evidence for anisotropy in the deep mantle beneath Alaska, *Geophys. Res. Lett*., *23,* 2417-2420.

Panning, M., and B. Romanowicz (2004), Inferences on flow at the base of earth's mantle based on seismic anisotropy, *Science*, *303*, 351-353.

Richards, M. A., and D. C. Engebretson (1992), Large-scale mantle convection and the history of subduction, *Nature*, *355*, 437-440.

Ritsema, J., and E. J. Garnero (1997), A strongly negative shear velocity gradient and lateral variability in the lowermost mantle beneath the Pacific, *J. Geophys, Res*., *102*, 20395-20411.

Silver, P. G., and W. W. Chan (1991), Shear wave splitting and subcontinental mantle deformation, *J. Geophys, Res*., *96*, 16429-16454.

Takeuchi, N., R. J. Geller, and P. R. Cummins (1996), Highly accurate P-SV complete synthetic seismograms using modified DSM operators, *Geophys. Res. Lett*., *23*, 1175-1178.

Tsuchiya, T., J. Tsuchiya, K. Umemoto and R. M. Wentzcovitch (2004a), Phase transition in $MgSiO_3$ perovskite in the earth's lower mantle, *Earth. Planet. Sci. Lett*., *224*, 241-248.

Tsuchiya, T., J. Tsuchiya, K. Umemoto and R. M. Wentzcovitch (2004b), Elasticity of post-perovskite $MgSiO_3$, *Geophys. Res. Lett*., *31*, L14603, doi:10.1029/2004GL020278.

Young, C. J., and T. Lay (1987), Evidence for a shear velocity discontinuity in the lower mantle beneath India and Indian Ocean, *Phys. Earth. Planet. Inter*, *49*, 37-53.

Young, C. J., and T. Lay (1990), Multiple phase analysis of the shear velocity structure in the D" region beneath Alaska, *J. Geophys, Res*., *95*, 17385-17402.

Figures

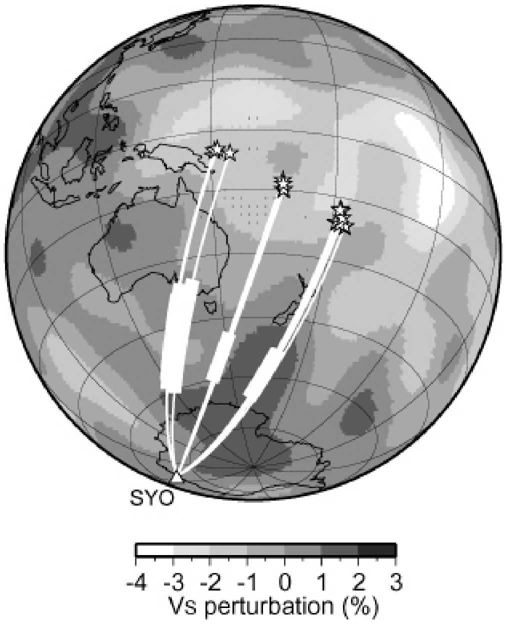

Figure 1 (Usui, Hiramatsu, Furumoto, Kanao, 2005)

Figure 1. The location of the events used in the Papua New Guinea and the Tonga-Kermadec regions (stars) and the Syowa station in Antarctica (SYO: triangle). Thin lines indicate direct S wave paths. Thick lines indicate portions of the paths in the D” layer for assumed D” layer thickness of 350km. Gray scale shows shear wave velocity perturbation at the depth of 2800km by Liu and Dziewonski [1998].

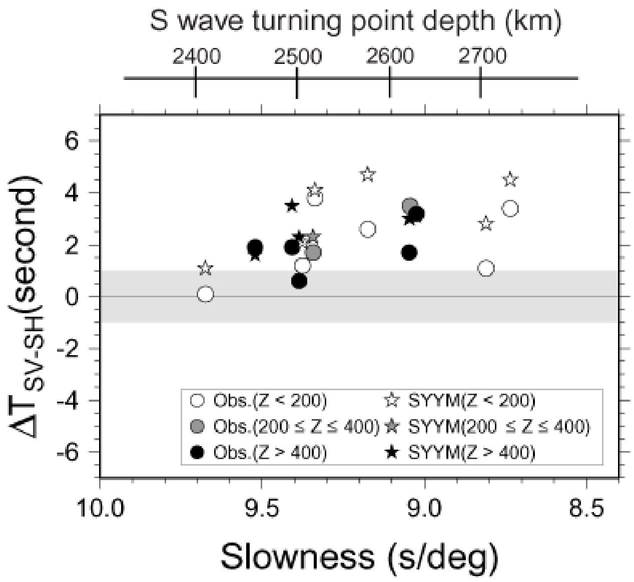

Figure 2 (Usui, Hiramatsu, Furumoto, Kanao, 2005)

Figure 2. A plot of the observed shear wave splitting (circles) and the predicted SYYM one (stars) demarked for different source depth intervals (Z, in km) versus the slowness of shear waves by PREM. The shaded region corresponds to SV-SH times within ±1.0s that represents the measurement error. A scale shown in the top is the depth of S wave turning point for PREM.

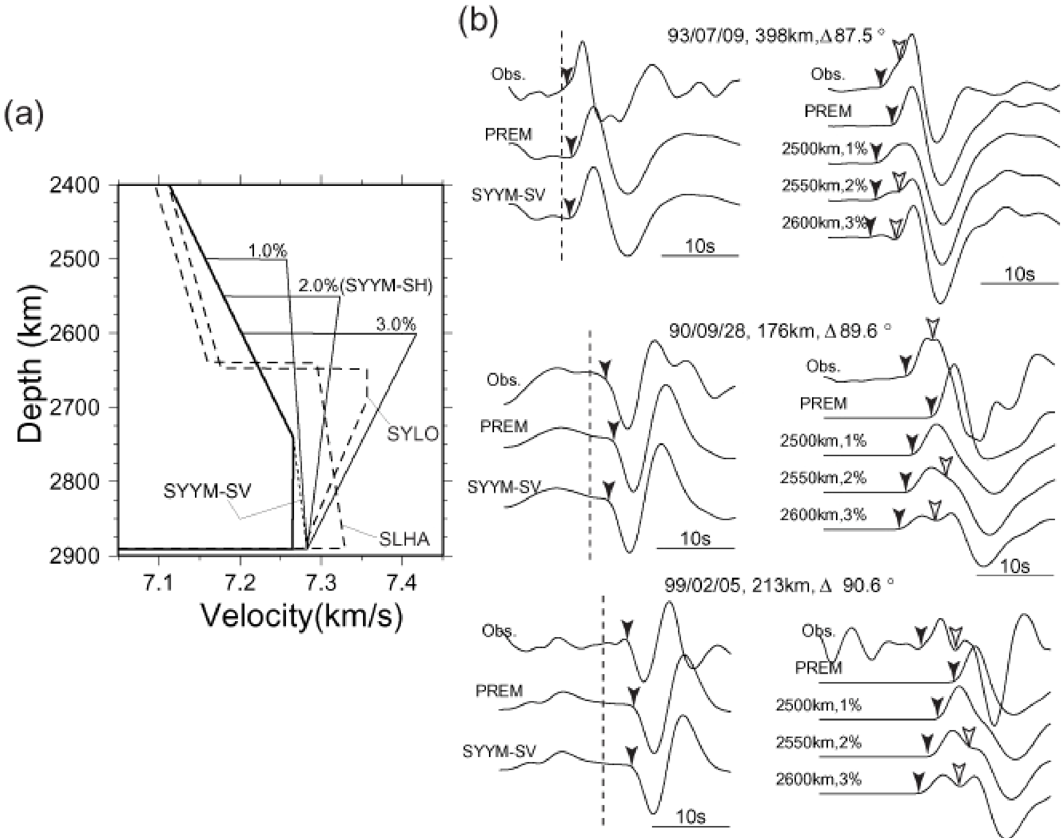

Figure 3 (Usui, Hiramatsu, Furumoto, Kanao, 2005)

Figure 3. (a) Velocity-depth profiles for models of SYYM, PREM and two regional models: SYLO beneath Alaska [Young and Lay, 1990] and SLHA beneath the Caribbean Sea [Lay and Helmberger, 1983]. Thick line is PREM and dash line is SYYM-SV model. Thin lines are three different discontinuity models for SH. The three models have a velocity jump of 1.0, 2.0, 3.0% at 2500, 2550, 2600km depth, respectively. (b) Comparison of observed waveforms and synthetics ones. We use SKS onset times to line up the each waveforms and maximum amplitude is normalized to unity, respectively. Inverse triangles are onset times for S and open ones are secondary

arrival. A vertical dash line on a SV trace shows the onset times of the observed SH arrival.